

# Very Light Axiguons and the Top Asymmetry

Gordan Z. Krnjaic<sup>1,2</sup>

1) *Theoretical Physics Department, Fermilab, Batavia, IL 60510, USA*

2) *Department of Physics and Astronomy, Johns Hopkins University, Baltimore, MD 21218, USA*

February 18, 2022

We show that very light (50 – 90 GeV) axiguons with flavor-universal couplings of order  $g_s/3$  may explain the anomalous top forward-backward asymmetry reported by both CDF and D0 collaborations. The model is naturally consistent with the observed  $t\bar{t}$  invariant mass distribution and evades bounds from light Higgs searches, LEP event shapes, and hadronic observables at the  $Z$  pole. Very light axiguons can appear as resonances in multijet events, but searches require sensitivity to masses below current limits.

## 1 Introduction

The CDF and D0 collaborations have recently reported measurements of the forward-backward asymmetry ( $A_{FB}$ ) in  $t\bar{t}$  production with intriguing deviations from the standard model prediction. CDF's result [1] in the lepton plus jets channel reports an inclusive parton level asymmetry

$$A_{FB}(\text{CDF})_{\ell j} = (15.8 \pm 7.4)\% \quad . \quad (1.1)$$

If their measurement in the dilepton channel [2] is combined with this result, the asymmetry becomes

$$A_{FB}(\text{CDF})_{\ell\ell+\ell j} = (20.9 \pm 6.6)\% \quad , \quad (1.2)$$

and exceeds the standard model prediction  $\simeq 5\%$  [3]-[5] by more than 2 standard deviations.

D0 performs a similar search [6] in the lepton plus jets channel and reports an inclusive parton-level asymmetry

$$A_{FB}(\text{D0})_{\ell j} = (19.6 \pm 6.5)\% \quad , \quad (1.3)$$

which is also more than  $2\sigma$  above the SM result. Taken together, these consistent deviations may be evidence for new physics in top quark production.

While all the inclusive measurements are consistent with each other, CDF's lepton plus jets search sees sharp mass dependence [1] in the binned result

$$\begin{aligned} A_{FB}(M_{t\bar{t}} < 450 \text{ GeV}) &= (-11.6 \pm 14.6)\% \quad , \\ A_{FB}(M_{t\bar{t}} > 450 \text{ GeV}) &= (47.5 \pm 11.4)\% \quad , \end{aligned}$$

where the high mass bin is  $3.4\sigma$  above the SM prediction. Neither D0 nor the complementary CDF dilepton search see the same effect; both find consistently positive  $> 2\sigma$  deviations from the SM over the full  $M_{t\bar{t}}$  range.

It has been observed that massive gluons with axial couplings can induce a large forward-backward asymmetry in  $t\bar{t}$  production by interfering with standard model processes [7]-[19]. Motivated primarily by the mass dependent CDF result, these models predict asymmetries that rise uniformly with invariant mass and feature a sign flip near  $M_{t\bar{t}} \approx 450$  GeV. Large (TeV scale) masses are typically required to satisfy dijet-resonance search bounds and suppress contributions to the  $t\bar{t}$  invariant mass distribution. To produce an asymmetry with the observed sign, most models also require flavor violation and are severely constrained [20] by limits on flavor changing neutral currents. For a comparison of heavy axiguons and other models that address the top asymmetry, see [21].

Relatively lighter axiguons (400 – 450 GeV) [22] can produce a large top asymmetry without flavor violation, but this mass scale is in tension with dijet resonance bounds and the differential  $M_{t\bar{t}}$  distribution. Extra field content is generally required to broaden decay widths and avoid resonant enhancements to top quark observables.

In this paper we propose a *very light* (50 – 90

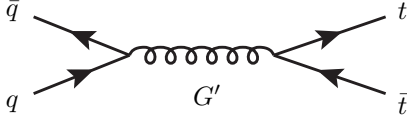


Figure 1: Axigluon contribution to  $t\bar{t}$  pair production. Interference with the standard model gluon exchange diagram generates  $\mathcal{A}_{int}^{G'}$ .

GeV), weakly coupled axigluon to explain the top asymmetry. The model inherits many of the features heavier axigluons enjoy, but counterintuitively avoids their experimental constraints by being light: dijet resonance searches suffer from large QCD backgrounds at low invariant masses, particles below the  $2m_t$  threshold do not produce bumps in the  $t\bar{t}$  invariant mass distribution, and nonresonant production suppresses new physics contributions to the  $t\bar{t}$  cross section, which start at fourth order in the axigluon coupling. We find that the strongest upper bounds in this mass range come from Tevatron searches for light Higgs bosons produced in association with an additional  $b$ -jet. The strongest lower bounds come from UA2 dijet searches and LEP measurements of the hadronic  $Z$  width.

In Section 2 we describe our model; in Section 3 we discuss the details of our numerical simulation; in Section 4 we address the experimental constraints; in Section 5 we compute the  $t\bar{t}$  forward-backward asymmetry and compare theoretical predictions with production-level data; in Section 6 we make some concluding remarks.

## 2 Model Description

We give the axigluon ( $G'$ ) flavor universal couplings to SM quarks

$$\mathcal{L} \supset g' G'_\mu{}^a \bar{Q} T^a \gamma^\mu \gamma^5 Q, \quad (2.1)$$

where  $g' \equiv \lambda g_s$  is the axigluon coupling constant, which we express in units of the strong coupling. This operator can arise from an extended  $SU(3)_1 \times SU(3)_2$  color group that breaks down to the diagonal  $SU(3)_c$  of QCD and gives rise to massive spin-1 color octets [23]-[26]. For an axigluon of mass  $m_{G'}$  our effective model requires a UV completion at the scale  $4\pi m_{G'}/g' = 1.7$  TeV and 850 GeV for  $\lambda = 0.3$  and 0.6 respectively. In this paper, we will focus

only on the low energy effective theory and leave UV model building for future work.

Without additional field content, all decays proceed through operator in Eq. (2.1), so axigluons can only decay to quark pairs and give rise to dijet and four jet events for single and pair production, respectively. Since we work in the regime where the axigluon is below the  $t\bar{t}$  threshold, the total width is [27]

$$\Gamma_{G'} = \frac{n_f}{6} \alpha_s \lambda^2 m_{G'} \quad , \quad (2.2)$$

where  $n_f$  is the number of active fermion flavors. For  $m_{G'} = 80$  GeV and  $\lambda = 0.4$ , this width is  $\Gamma_{G'} \simeq 1.1$  GeV.

The differential cross section for the process  $q\bar{q} \rightarrow t\bar{t}$  in the CM frame is a sum of standard model, interference, and axigluon terms

$$\frac{d\hat{\sigma}(G')}{d\cos\theta} = \mathcal{A}_{SM} + \mathcal{A}_{int}^{G'} + \mathcal{A}_{axi}^{G'} \quad , \quad (2.3)$$

where [28]

$$\mathcal{A}_{SM} = \frac{\pi \alpha_s^2 \beta}{9 \hat{s}} \left( 2 - \beta^2 + (\beta \cos\theta)^2 \right) \quad , \quad (2.4)$$

$$\mathcal{A}_{int}^{G'} = \frac{4\pi \alpha_s^2 \lambda^2}{9} \frac{(\hat{s} - m_{G'}^2) \beta^2 \cos\theta}{(\hat{s} - m_{G'}^2)^2 + m_{G'}^2 \Gamma_{G'}^2} \quad , \quad (2.5)$$

$$\mathcal{A}_{axi}^{G'} = \frac{\pi \alpha_s^2 \lambda^4}{9} \frac{\hat{s} \beta^3 (1 + \cos^2\theta)}{(\hat{s} - m_{G'}^2)^2 + m_{G'}^2 \Gamma_{G'}^2} \quad . \quad (2.6)$$

Here  $\beta \equiv \sqrt{1 - 4m_t^2/\hat{s}}$  is the top quark velocity and  $\theta$  is the angle between the incoming quark and outgoing top in the CM frame. A forward-backward asymmetry can only arise from terms with odd powers of  $\cos\theta$ , so the effect is due entirely to interference. In the presence of both vector and axial-vector couplings, there is an additional small contribution to the asymmetry from the new-physics squared term.

Note that the asymmetry generating term  $\mathcal{A}_{int}^{G'}$  is proportional to  $(\hat{s} - m_{G'}^2)$ . For heavier axigluons, this dependence gives rise to a negative asymmetry because the mass is typically larger than the partonic CM energy. To compensate, many models introduce opposite sign couplings to the first and third generations. In our case,  $m_{G'} < \hat{s}$  for on-shell  $t\bar{t}$  production, so the asymmetry is always positive and flavor violation is unnecessary.

### 3 Simulation and Acceptances

In the lepton plus jets analysis, CDF unfolds raw data by deconvolving their detector simulation and jet algorithm to yield a partonic data set from events that survive cuts at the detector level. To compare our model predictions with this data, it is necessary to generate an event sample with partonic  $t\bar{t}$  pairs in the final state. However, knowing the predicted cross section and experimental luminosity is not enough to properly normalize kinematic distributions from the partonic simulation; we must also know the detector level acceptances. We thus perform two simulations: one at the partonic level to make our plots and one at the detector level with CDF’s cuts to compute the acceptances that normalize these distributions.

We simulate the partonic process  $p\bar{p} \rightarrow t\bar{t}$  in MadGraph 5 [29] using a model file generated with FeynRules [30]. This file adds the operator in Eq. (2.1) to the full standard model Lagrangian so that the process in Figure 1 contributes to  $t\bar{t}$  production and gives rise to interference with SM gluon-exchange.

For the acceptances, we also perform a more realistic simulation ( $p\bar{p} \rightarrow t\bar{t} \rightarrow \ell\nu + 4j$ ) using PYTHIA [31] for the parton shower and PGS [32] for detector effects. To compare with CDF’s lepton plus jets search, we impose the following cuts: at least four jets with  $E_T > 20$  GeV and at least one  $b$ -tag; for non- $b$  jets  $|\eta_j| < 2$ , for  $b$ -jets  $|\eta_{bj}| < 1$ ; large missing energy  $\cancel{E}_T > 20$  GeV; and exactly one electron or muon with  $p_T^\ell > 20$  GeV and  $|\eta_\ell| < 1$ .

Note that there is some error introduced by this approximate method. A complete comparison with experimental data would not only run a full detector simulation (including PYTHIA and PGS), but also identify top quarks with a least-squares kinematic fit and unfold the detector-level output using the CDF algorithm that reconstructs partonic events from raw data. Nonetheless, our approach accurately reproduces CDF’s standard model expectation for the  $t\bar{t}$  invariant mass distribution<sup>1</sup> so the error introduced by a constant acceptance function

<sup>1</sup> Although the forward-backward asymmetry arises only at loop level in the SM, its numerical value is tiny ( $\sim 5\%$ ), so this tree level method also adequately reproduces the (nearly symmetric) SM predictions for the  $\Delta y = y_t - y_{\bar{t}}$  rapidity distributions in [1].

is likely to be small in our case as well. We leave the full unfolding for future work.

### 4 Experimental Constraints

Models that explain the top asymmetry must agree with the  $t\bar{t}$  invariant mass distribution and total cross section, both of which are in good agreement with standard model predictions. Any candidate model with an  $s$ -channel mediator must satisfy constraints from dijet resonance searches at hadron colliders. In our case, we must also contend with a variety of older measurements that set lower bounds on new colored particles.

#### 4.1 Top Quark Measurements

The  $t\bar{t}$  cross section at the Tevatron has been measured to be  $\sigma_{t\bar{t}}^{\text{exp.}} = 7.50 \pm 0.48$  pb [33], which agrees with the standard model prediction in perturbative QCD<sup>2</sup>,  $\sigma_{t\bar{t}}^{\text{sm}} \simeq (6.32 - 7.99)$  pb for  $m_t = 172$  GeV [34]. The leading order result,  $(\sigma_{t\bar{t}}^{\text{sm}})_{\text{LO}} \simeq 5.63$  pb, computed with MadGraph, implies a SM  $K$ -factor between 1.12 and 1.42.

Including an axigluon with  $m_{G'} = 80$  GeV and  $\lambda = 0.4$ , gives a total LO cross section of  $(\sigma_{t\bar{t}}^{\text{axi}})_{\text{LO}} = 6.08$  pb, which is only an 8% increase over the SM LO result. This minor enhancement is due entirely to  $\mathcal{A}_{axi}^{G'}$  in Eq.(2.1), which is fourth order in the axigluon coupling; the interference term  $\mathcal{A}_{int}^{G'}$  does not contribute to the total cross section. Although computing higher order corrections is beyond the scope of this work, the color structure of the axigluon exchange diagrams is identical to that of the relevant SM processes, so we expect higher order corrections to be of similar magnitude, though a more precise calculation is necessary to take into account the additional interference. As long as the  $K$  factor does not differ substantially from that of SM production, the total  $t\bar{t}$  cross section stays in good agreement with experiment. For the remainder of this paper, we will assume the  $K$  factor to be 1.2, so our benchmark cross section becomes 7.3 pb.

For very light axigluons ( $m_{G'} \ll 2m_t$ ), top pair production is nonresonant, so the invariant mass distribution is also in good agreement with experiment. In Figure 2 we show the simulated  $M_{t\bar{t}}$  distribution

<sup>2</sup> For complementary calculations see [35, 36].

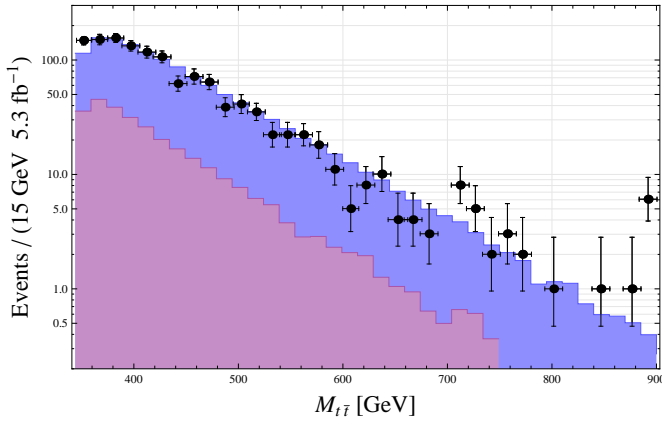


Figure 2: Tevatron invariant mass distribution for  $t\bar{t}$  pairs (blue, color online) including both axigluon and background contributions. Data points and standard model background (purple) are taken from CDF’s lepton plus jets search [1]. Here we use  $\lambda = 0.4$  and  $m_{G'} = 80$  GeV. After including a  $K$ -factor of 1.2, the top cross section is  $\sigma_{t\bar{t}} = 7.3$  pb. Applying the CDF cuts (see Section 3) gives an acceptance of 2.6%.

(blue) plotted alongside the CDF data points and standard model background (purple) taken from the lepton plus jets search [1].

## 4.2 Dijet Resonance Searches

Quark coupled axigluons give rise to two and four jet events from single and pair production, respectively. Our mass range of interest (50 – 90 GeV) is safe from Tevatron [37, 38] and LHC [39, 40] dijet resonance searches, which do not set bounds on masses below 180 and 200 GeV, respectively. A preliminary ATLAS analysis of multijet events [41] sets limits on color octet scalars with narrow widths, but does not constraint masses below 100 GeV. With lower search thresholds, this model may be testable at both the Tevatron and LHC, however, signal and background are expected to be large at both colliders [42].

The UA2 search for hadronic  $W$  and  $Z$  decays [43] measures the exclusive two-jet mass spectrum between 48 and 300 GeV, which constrains the light axigluon parameter space. Using  $4.7 \text{ pb}^{-1}$  for  $M_{jj} > 66$  GeV (and  $0.58 \text{ pb}^{-1}$  for  $48 \text{ GeV} < M_{jj} < 66$  GeV), the combined  $W$  and  $Z$  resonances are extracted with a bi-gaussian fit above a smooth background function normalized to the data. The best fit

bi-gaussian signal spans the  $M_{jj}$  range between 70 and 100 GeV and yields a cross section of  $\sigma \cdot \mathcal{B}r(W, Z \rightarrow jj)_{\text{obs.}} = 9.6 \pm 2.3 \pm 1.1 \text{ nb}$ , whose central value exceeds the SM prediction at NLO,  $\sigma \cdot \mathcal{B}r(W, Z \rightarrow jj)_{\text{SM}} = 5.8 \text{ nb}$ , by almost a factor of two.

Although a three-gaussian fit and a QCD background prediction are necessary to properly constrain axigluons using this data, we can extract a rough bound by finding  $(\lambda, m_{G'})$  values for which the combined SM and new-physics predictions exceed the observed number of events under the best fit gaussian by  $2\sigma$ . In Figure 3 we plot the exclusion boundary (yellow dot-dashed line) determined using Madgraph, PYTHIA, and PGS to simulate our signal.

For dijet masses below 70 GeV, the UA2 analysis does not attempt to fit any signal, so a possible resonance would almost certainly have been missed given the very large background in this mass range. Even near  $m_W$  and  $m_Z$ , the signal/background ratio is only a few percent and the gauge boson peak is not visible to the naked eye (see Figure 5 in [43]) prior to a rescaling that emphasizes the region around the known  $W$  and  $Z$  masses. Since the background model for this search is purely data-driven, the low-mass region does not impose a meaningful constraint without a dedicated bump hunt.

## 4.3 Light Higgs Searches

Tevatron searches that look for light Higgs bosons produced in association with  $b$ -jets ( $p\bar{p} \rightarrow h\bar{b} \rightarrow b\bar{b}b$ ) are sensitive to axigluon decays into  $b$ -quarks. Since these searches require at least three  $b$ -tags to reduce the QCD multijet background, the bounds they impose on  $\sigma(h\bar{b}) \cdot \mathcal{B}r(h \rightarrow b\bar{b})$  also apply to the processes  $p\bar{p} \rightarrow G'\bar{b} \rightarrow b\bar{b}b$  and  $p\bar{p} \rightarrow G'bb \rightarrow b\bar{b}bb$ , the latter of which can also arise from pair produced axigluons. However, the CDF [44] and D0 [45] results only apply to masses above 90 GeV; light axigluons fall below the sensitivity threshold. To be conservative, we will only consider masses below 90 GeV where the  $3b$  constraints do not apply.

The authors in [46] use Tevatron Higgs searches in the associated production channel,  $p\bar{p} \rightarrow Wh \rightarrow (\ell\nu)(b\bar{b})$  to exclude axigluons with  $\lambda = 1$  between 75 – 125 GeV assuming  $\mathcal{B}r(G' \rightarrow b\bar{b}) = 1/5$ . In our case with  $\lambda = 0.4$ , the Tevatron  $q\bar{q} \rightarrow WG'$  cross section decreases by a factor of  $\lambda^2$ , which reduces

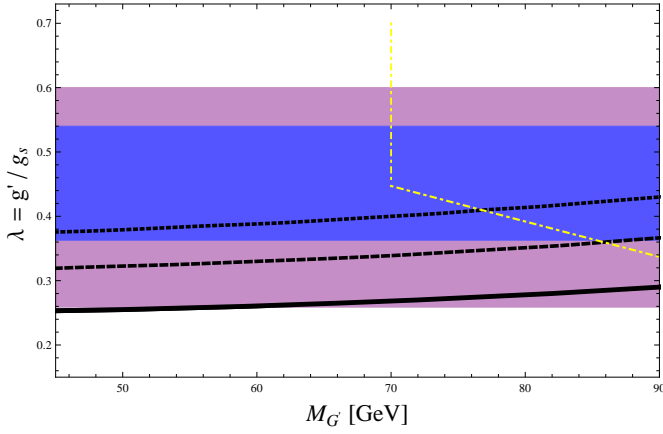


Figure 3: Allowed axigluon parameter space in the  $(\lambda, m_{G'})$  plane plotted alongside bounds from dijet-resonance searches and  $\Gamma(Z \rightarrow \text{hadrons})$  measurements assuming different extractions of  $\alpha_s$ . The blue and purple bands (color online) are regions favored by the combined CDF/D0 inclusive asymmetry measurements at  $1\sigma$  and  $2\sigma$ , respectively. The dot-dashed yellow curve marks the approximate  $2\sigma$  bound above which model predictions exceed UA2 dijet limits from hadronic  $W$  and  $Z$  decays (see Section 4.2). The solid black curve marks the boundary above which corrections to the hadronic  $Z$  width exceed the observed value by  $2\sigma$  assuming the standard model extraction of  $\alpha_s(m_Z) = 0.1184$ . The dashed and dotted black curves give the same bound, but respectively assume 2.5% and 5% reductions to the SM value of  $\alpha_s(m_Z)$ . Reductions of this magnitude are typical of light axigluon contributions to the QCD beta function (for a discussion see Sections 4.5 and 4.6). The region above  $m_{G'} > 90$  GeV is excluded by Tevatron 3b-searches. Since LEP event shapes rule out gluon-coupled adjoint fermions around 50 GeV, our model may encounter a stronger lower bound since axigluons also couple to quarks, but a proper analysis is necessary to set the correct limit.

the axigluon signal  $\sigma \cdot \mathcal{B}r$  from  $\approx 50$  pb down to  $\approx 5$  pb for  $m_{G'} = 50$  GeV also assuming  $\mathcal{B}r(G' \rightarrow b\bar{b}) = 1/5$ . This falls safely below the quoted bound of  $\lesssim 20$  pb, however, this number is based on analysis from an unpublished talk, so its status is not clear. Current Tevatron searches for the associated production of Higgs bosons are not sensitive to masses below 100 GeV [47, 48].

Naively it would appear that LEP searches in the

Higgstrahlung channel [49]–[52]  $e^+e^- \rightarrow Zh \rightarrow 4j$  would be sensitive to light axigluons produced in  $e^+e^- \rightarrow Z^* \rightarrow q\bar{q}G' \rightarrow 4j$  events. However, the event selection algorithms in these analyses look for kinematics that fit the Higgstrahlung topology in which the invariant masses of jet pairs produce both  $Z$  and Higgs resonances. In events with on-shell axigluons, all four jets arise from virtual  $Z$  exchange, so this possibility is highly disfavored. Furthermore, this process occurs at order  $\lambda^2$  and suffers additional phase-space suppression.

Similar considerations apply to LEP measurements of triple gauge boson couplings [53]–[56] which look for  $e^+e^- \rightarrow W^+W^-$ ,  $ZZ \rightarrow 4j$  events. These analyses select events using neural network algorithms designed to identify diboson production; light axigluons arising from  $Z$  exchange have very different kinematics and fail this selection, which requires some combination of jet pairs to reconstruct at least one gauge boson mass. At the higher end of our mass range ( $m_{G'} > 80$  GeV) it may be possible for an axigluon to fake a hadronically decaying SM gauge boson, but the other two jets would not reconstruct a resonance. The coupling and phase-space suppression also diminish the rate at these searches, so axigluon production is negligible compared to tree-level diboson and QCD background processes.

#### 4.4 Event Shapes

Constraints on light colored-particles have been extracted from the analysis of event shapes at LEP. Comparing multijet data with calculations in soft colinear effective theory (SCET) rules out color adjoint fermions below 51 GeV at 95% confidence [57]. However, this approach assumes that the new field couples only to gluons, with no tree-level quark interactions. To set a proper lower bound, it is necessary to repeat this analysis with more general assumptions, however, it is unlikely that this would yield a more lenient limit so we will not consider masses below  $\approx 50$  GeV.

LEP studies of four-jet events from  $Z$  decays [58]–[61] can be sensitive to light, colored particles that couple to quarks. Various angular distributions are used to successfully distinguish  $SU(3)_c$  QCD from alternative abelian theories of the strong force, so the presence of light axigluons could potentially

spoil this success. However, using Madgraph to generate four-jet  $Z$  decays at the parton level, we find that the presence of an axigluon ( $\lambda = 0.4$ ) in our mass range does not qualitatively distort these angular distributions relative to the QCD prediction. This is unsurprising since  $\mathcal{O}(10\%)$  of SM hadronic  $Z$  decays produce four-jets – the exact number depends on  $y_{cut}$  and other jet algorithm details [62] – whereas in our model only  $\mathcal{O}(0.1\%)$  of hadronic decays proceed through  $Z \rightarrow q\bar{q} G' \rightarrow 4j$  prior to imposing cuts (see Section 4.6). For higher energies probed by LEP II ( $\sqrt{s} \approx 200$  GeV), the total  $e^+e^- \rightarrow Z^* \rightarrow q\bar{q}G' \rightarrow 4j$  rate is similarly negligible compared to SM four jet production; this conclusion is robust for values of  $y_{cut}$  spanning several orders of magnitude.

#### 4.5 Running of $\alpha_s$

Since axigluons couple to the strong sector, they give rise to loop diagrams that modify the QCD beta function above the scale  $m_{G'}$ . The standard model running between energy scales  $Q$  and  $\mu$  is given by

$$\alpha_s(Q^2) = \frac{\alpha_s(\mu^2)}{1 + b \alpha_s(\mu^2) \log\left(\frac{Q^2}{\mu^2}\right)} \quad , \quad (4.1)$$

where, to leading order,  $b = (33 - 2n_f)/12\pi$  and  $n_f$  is the number of active flavors. Since axigluons have the same quantum numbers and self couplings as gluons, their principal effect on the running is to double the gluon contribution to the beta function above  $m_{G'}$ :  $b \rightarrow (2 \times 33 - 2n_f)/12\pi$ . This accelerates asymptotic freedom and yields smaller values of  $\alpha_s$  near the weak scale.

While this adjustment naïvely jeopardizes the agreement between theory and experiment for the running, the experimental extraction of  $\alpha_s$  depends entirely on the assumed validity of standard model QCD with no additional field content [63]. At each energy scale, an  $\alpha_s$ -dependent observable is equated to the SM prediction and the resulting data point is extracted implicitly. If light new states were present in the strong sector, this data would completely ignore their contributions, so the current agreement between theory and experiment does not constrain our model.

To roughly estimate the axigluon correction to  $\alpha_s(m_Z)$ , we use a well-measured value of  $\alpha_s$  below

$m_{G'}$  as an IR boundary condition and evolve it with the new beta function. This method is crude because even low-energy observables used to extract  $\alpha_s$  depend somewhat on virtual axigluon processes, which are ignored in the extraction of reported measurements. Nonetheless, using the boundary condition  $\alpha_s(14.9 \text{ GeV}) = 0.160$ , [63] the weak-scale value becomes  $\alpha_s(m_Z) = 0.105, 0.110$ , and  $0.115$  for  $m_{G'} = 50, 65$  and  $80$  GeV, respectively. Different IR boundary conditions give similar downward corrections of order a few percent relative to the SM extraction  $\alpha_s(m_Z) = 0.1184$ . Note that this result is independent of  $\lambda$  since axigluons couple to gluons with QCD strength.

This model also predicts a kink in the running of  $\alpha_s$  near  $m_{G'}$ . Our mass range of interest (50 – 90 GeV), however, overlaps with a region where data points are sparsely distributed with relatively large error bars (see Figure 6 in [63]) compared to the data set as a whole. Kinks in the slope of  $\alpha_s$  would, therefore, be unlikely to stand out in the data. Nonetheless, a model-dependent extraction of  $\alpha_s$  is necessary to evaluate the possibility of kinks or overall data shifts due to new physics contributions.

#### 4.6 Hadronic $Z$ Width

The strongest lower bound on  $m_{G'}$  comes from virtual and three-body corrections to the hadronic  $Z$  width. Axigluons that couple to quarks with QCD strength ( $\lambda = 1$ ) enhance this width by a factor of

$$1 + \frac{\alpha_s}{\pi} f(m_Z/m_{G'}) + \mathcal{O}(\alpha_s^2) \quad , \quad (4.2)$$

where  $f$  is a function derived in [64, 65]. The LEP measurement of  $\Gamma(Z \rightarrow \text{hadrons})$  and the extracted value of  $\alpha_s(m_Z)$  constrain the size of  $f(m_Z/m_{G'})$  and severely restrict axigluon masses:  $m_{G'} > 570$  (365) GeV for  $\lambda = 1$  at the 65% (95%) confidence level [46].

However,  $f$  is highly nonlinear, so the mass constraint is *extremely* sensitive to the axigluon coupling. In our scenario, the constraint on  $f$  applies to the combination  $\lambda^2 f$ , which dramatically weakens the lower bound on  $m_{G'}$ . Furthermore, following the discussion in Section 4.5, light axigluon ( $m_{G'} < m_Z$ ) contributions to the QCD beta function generically decrease the value of  $\alpha_s(m_Z)$  at the percent level. Since this is used to compute QCD corrections to the



SM prediction for  $\Gamma(Z \rightarrow \text{hadrons})$  [66], a smaller value opens up more allowed parameter space for new physics; the positive axigluon contribution to the width compensates for a slightly smaller SM result which is reduced by the new value of  $\alpha_s$ .

In Figure 3 we plot  $2\sigma$  exclusion bounds from the hadronic  $Z$  width on the  $(\lambda, m_{G'})$  plane alongside the regions favored by combined CDF and D0  $A_{FB}$  measurements (discussed in Section 5). The solid black curve uses the standard model extraction  $\alpha_s(m_Z) = 0.1184 \pm 0.0007$  [63] and the measured  $\Gamma(Z \rightarrow \text{hadrons}) = 1.744 \pm 0.002$  GeV [67] to identify parameters for which the theoretical prediction exceeds the measured central value by  $2\sigma$ . Also plotted are the  $2\sigma$  bounds assuming 2.5 % (black dashed) and 5% (black dotted) reductions in  $\alpha_s(m_Z)$  due to the modified running that includes axigluon contributions. These curves show how sensitive the bound is to modifications in  $\lambda$  and  $\alpha_s(m_Z)$ . Since we generically expect light axigluons to reduce the value of  $\alpha_s(m_Z)$  by a few percent relative to the SM extraction, the dashed and dotted curves are more faithful to the underlying physics. Given the sensitivity of the bound, a proper extraction of  $\alpha_s$  involving axigluon processes is necessary to accurately constrain the parameter space; the limits in Figure 3 serve merely to illustrate the impact on the allowed region.

#### 4.7 Bounds from $\sigma(e^+e^- \rightarrow \text{hadrons})$

The authors in [64] calculate <sup>3</sup> axigluon corrections to the ratio

$$R(s) \equiv \frac{\sigma(e^+e^- \rightarrow \text{hadrons})}{e^4/12\pi s} \quad (4.3)$$

at the scale  $\sqrt{s} = 34$  GeV and thereby exclude masses below 50 GeV at 95% confidence assuming  $\lambda = 1$ . As with the hadronic  $Z$  width, the corrections for this process are proportional to the factor in Eq.(4.2) with the replacement  $\alpha_s \rightarrow \lambda^2 \alpha_s$ , so the discussion in Section 4.6 applies to this bound as well. Since  $\Gamma(Z \rightarrow \text{hadrons})$  is extracted from  $R$  data at the  $Z$  pole, the allowed parameter space in Figure 3 is automatically consistent with bounds from  $R$  near  $\sqrt{s} = m_Z$ . For smaller energies in our

<sup>3</sup>Note that [64] corrects some minor, yet consequential errors from an earlier paper [65] that placed a far stronger lower-bound on the mass.

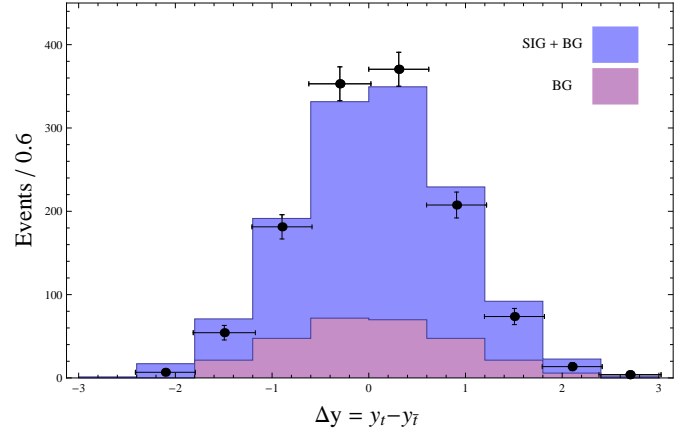


Figure 4: Inclusive top anti-top rapidity difference distribution plotted against unfolded CDF data. Here we use the same model parameters as in Fig. 2. The blue histograms include both signal and standard model background. Both data and background (purple) are taken from [1]. This plot omits the small, loop level asymmetry generated by SM processes.

range of interest,  $\sqrt{s} \in 50 - 90$  GeV, the uncertainties on the  $R$  data are larger than those at the  $Z$  pole [67], so the bound is weaker.

## 5 Forward Backward Asymmetry

The forward-backward asymmetry can be written

$$A_{FB} \equiv \frac{N(\Delta y > 0) - N(\Delta y < 0)}{N(\Delta y > 0) + N(\Delta y < 0)} \quad , \quad (5.1)$$

where  $\Delta y \equiv y_t - y_{\bar{t}}$  is the rapidity difference between the top and anti-top quarks.

In Figure 3 we show the favored parameter space in the  $(\lambda, m_{G'})$  plane. The blue (purple) band represents the region of  $1\sigma$  ( $2\sigma$ ) agreement with the combined CDF, Eq. (1.2), and D0, Eq.(1.3) inclusive measurements. For typical points in these regions, the model predicts a positive asymmetry of order 20%.

In Figure 4 we show the inclusive  $t\bar{t}$  rapidity-difference distribution plotted against the CDF data. The signal simulation is identical to that used to generate Figure 2 with  $m_{G'} = 80$  GeV and  $\lambda = 0.4$ . After applying the cuts described in Section 3, the acceptance is 2.6%. This plot only depicts the effects of tree-level processes; the histograms do not include the small asymmetry induced by standard

model processes. However, the numerical results in Fig. 3 include the full asymmetry with both SM and new physics contributions.

Although our simulation gives an acceptable fit to the rapidity data, some of the bins are more than  $1\sigma$  away from data points. We, however, do not expect perfect agreement at this level of analysis. The distribution in Figure 4 is a rough approximation of the full theory prediction which requires both a full CDF detector simulation and the subsequent unfolding for a proper comparison with data.

In Figure 5 we show the theory prediction for the mass dependent asymmetry  $A_{FB}(M_{t\bar{t}})$  plotted alongside the unfolded CDF data. Like other light  $s$  channel mediators, light axigluons predict a positive asymmetry throughout the whole range of invariant masses. While the agreement at low invariant mass is not ideal, neither D0 nor the CDF dilepton measurement observe strong mass dependence, so the significance of the mass-dependent data is not clear.

Note that in Figures 2, 4 and 5 we only compare the model to CDF results because their published distributions feature production-level data, which allow for a direct comparison with parton level simulations. Comparison with D0's distributions requires a detailed understanding of their detector simulation, which is beyond the scope of this work. Our conclusions have emphasized inclusive results from both collaborations since these are in better agreement with each other than the more controversial mass-dependent data.

## 6 Conclusions

We have shown that a light axigluon with flavor universal couplings can generate a large, positive  $t\bar{t}$  asymmetry and naturally agrees with measurements of  $d\sigma/dM_{t\bar{t}}$ . The model has viable parameter space consistent with light Higgs bounds, dijet resonance searches and measurements of the hadronic  $Z$  width.

For masses between  $50 - 90$  GeV and quark couplings in the range  $0.3 g_s - 0.6 g_s$ , the theoretical prediction for the parton-level top asymmetry is in good agreement with inclusive results from both CDF and D0. The asymmetry is proportional to  $(\hat{s} - m_{G'}^2)$ , so the sign of  $A_{FB}$  is always positive for on shell top pair production with  $\sqrt{s} > 2m_t \gg m_{G'}$ .

In the presence of a light axigluon, both the pre-

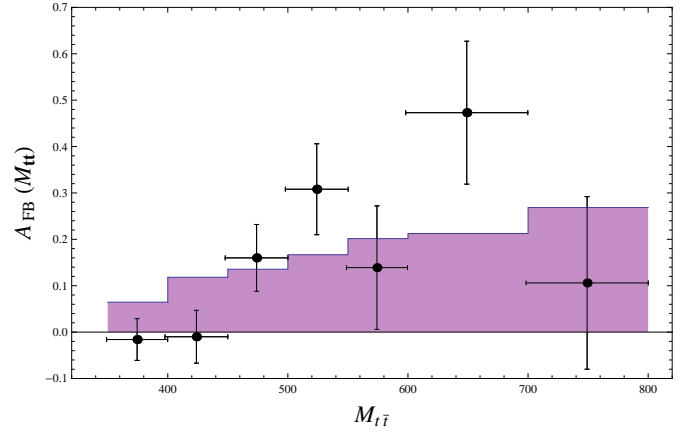


Figure 5: Theory prediction for the mass dependent  $t\bar{t}$  asymmetry (purple histograms) plotted against the binned, unfolded CDF data in the lepton plus jets channel [1]. Here we use the same model parameters as in Fig. 2. For comparison with CDF, the bin sizes are 50 GeV for  $M_{t\bar{t}} < 600$  GeV and 100 GeV for larger invariant masses. Since the interference term in the differential cross section, Eq. (2.5), is proportional to  $(\hat{s} - m_{G'}^2)$ , the asymmetry is always positive for on-shell  $t\bar{t}$  production. This is a generic feature of light axigluon models.

dicted and observed values of  $\alpha_s$  are modified at the percent level. A reanalysis of  $\alpha_s(\sqrt{s})$  measurements could reveal small downward shifts in the data since the modified beta function accelerates the running of  $\alpha_s$  in the presence of an axigluon. The downward shift in  $\alpha_s$  also decreases the SM predictions for  $\Gamma(Z \rightarrow \text{hadrons})$  and  $\sigma(e^+e^- \rightarrow \text{hadrons})$ , which expands the parameter space for  $(\lambda, m_{G'})$  values that explain the top asymmetry.

Although the QCD background at low masses is formidable, it may be possible to revisit UA2 dijet data and perform a dedicated bump hunt in the low mass region with updated background calculations. It should also be possible to include light axigluons in a SCET reanalysis of event shapes in LEP data, which would likely set the strongest lower bound on this model.

If very light axigluons explain the top forward-backward asymmetry, the Tevatron and LHC experiments should, in principle, be able to observe resonances in two and four jet events from single and pair production. Since the effective model presented in this paper demands a UV completion at energy scales near the LHC's designed sensitivity,



we predict new physics around the TeV scale, but the specific signals are model dependent at this level of description and would be interesting to pursue as future work.

**Acknowledgments:** We thank Johan Alwall, Bogdan Dobrescu, David Fehling, Patrick Fox, Graham Kribs, Roni Harnik, David E. Kaplan, Martin Schmaltz, Daniel Stolarski, and Morris Swartz for helpful discussions. GZK is supported by a Fermilab Fellowship in Theoretical Physics and by the National Science Foundation under grant number 106420. Fermilab is operated by Fermi Research Alliance, LLC, under Contract DE-AC02-07-CH11359 with the US Department of Energy.

## References

- [1] T. Aaltonen *et al.* [CDF Collaboration], Phys. Rev. **D83**, 112003 (2011), [[arXiv:1101.0034](#)].
- [2] CDF Public Note, [10436].
- [3] J. H. Kuhn and G. Rodrigo, Phys. Rev. D **59**, 054017 (1999), [[arXiv:9807420](#)].
- [4] V. Ahrens, A. Ferroglia, M. Neubert, B. D. Pecjak and L. L. Yang, [[arXiv:1106.6051](#)].
- [5] M. T. Bowen, S. D. Ellis, D. Rainwater, Phys. Rev. **D73**, 014008 (2006), [[arXiv:0509267](#)].
- [6] D0 Collaboration, [[arXiv:1107.4995](#)].
- [7] O. Antunano, J. H. Kuhn and G. Rodrigo, Phys. Rev. D **77**, 014003 (2008), [[arXiv:0709.1652](#)].
- [8] P. H. Frampton, J. Shu and K. Wang, Phys. Lett. B **683**, 294 (2010), [[arXiv:0911.2955](#)].
- [9] M. Bauer, F. Goertz, U. Haisch, T. Pfoh, S. Westhoff, JHEP **1011**, 039 (2010), [[arXiv:1008.0742](#)].
- [10] Y. Bai, J. L. Hewett, J. Kaplan and T. G. Rizzo, JHEP **1103**, 003 (2011), [[arXiv:1101.5203](#)].
- [11] A. R. Zerwekh, [[arXiv:1103.0956](#)].
- [12] B. Xiao, Y. k. Wang and S. h. Zhu, [[arXiv:1011.0152](#)].
- [13] X. P. Wang, Y. K. Wang, B. Xiao, J. Xu and S. H. Zhu, Phys. Rev. D **83**, 115010 (2011), [[arXiv:1104.1917](#)].
- [14] H. Wang, Y. K. Wang, B. Xiao and S. H. Zhu, [[arXiv:1107.5769](#)].
- [15] J. A. Aguilar-Saavedra and M. Perez-Victoria, [[arXiv:1107.2120](#)].
- [16] E. Gabrielli, M. Raidal, [[arXiv:1106.4553](#)].
- [17] R. Barcelo, A. Carmona, M. Masip, J. Santiago, Phys. Rev. D *in press* [[arXiv:1105.3333](#)].
- [18] R. Barcelo, A. Carmona, M. Masip, J. Santiago, [[arXiv:1106.4054](#)].
- [19] E. Alvarez, L. Da Rold, J. I. S. Vietto and A. Szyrkman, [[arXiv:1107.1473](#)].
- [20] R. S. Chivukula, E. H. Simmons and C. P. Yuan, Phys. Rev. D **82**, 094009 (2010), [[arXiv:1007.0260](#)].
- [21] M. I. Gresham, I. W. Kim, K. M. Zurek, Phys. Rev. **D83**, 114027 (2011), [[arXiv:1103.3501](#)].
- [22] G. Tavares, M. Schmaltz [[arXiv:1107.0978](#)].
- [23] L. J. Hall and A. E. Nelson, Phys. Lett. B **153**, 430 (1985), [Journal Server].
- [24] P. H. Frampton, S. L. Glashow, Phys. Lett. **B190**, 157 (1987). [Journal Server].
- [25] C. T. Hill, S. J. Parke, Phys. Rev. **D49**, 4454-4462 (1994), [[arXiv:hep-ph/9312324](#)].
- [26] C. T. Hill, Phys. Lett. **B266**, 419-424 (1991), [Journal Server].
- [27] P. Ferrario and G. Rodrigo, Phys. Rev. D **78**, 094018 (2008), [[arXiv:0809.3354](#)].
- [28] Q. H. Cao, D. McKeen, J. L. Rosner, G. Shaughnessy, C. E. M. Wagner, Phys. Rev. **D81**, 114004 (2010), [[arXiv:1003.3461](#)].
- [29] J. Alwall, M. Herquet, F. Maltoni, O. Mattelaer, T. Stelzer, [[arXiv:1106.0522](#)].
- [30] N. D. Christensen, C. Duhr, Comput. Phys. Commun. **180**, 1614-1641 (2009), [[arXiv:0806.4194](#)].

- [31] T. Sjostrand, S. Mrenna and P. Skands, JHEP **0605**, 026 (2006), [[arXiv:0603175](#)].
- [32] J. S. Conway, Pretty Good Simulation (PGS).
- [33] CDF Public Note, [9913].
- [34] S. Moch, P. Uwer, Phys. Rev. **D78**, 034003 (2008), [[arXiv:0804.1476](#)].
- [35] N. Kidonakis and R. Vogt, Phys. Rev. D **78**, 074005 (2008), [[arXiv:0805.3844](#)].
- [36] M. Cacciari, S. Frixione, M. L. Mangano, P. Nason and G. Ridolfi, JHEP **0809** (2008) 127, [[arXiv:0804.2800](#)].
- [37] T. Aaltonen *et al.* [CDF Collaboration], Phys. Rev. D **79**, 112002 (2009), [[arXiv:0812.4036](#)].
- [38] V. M. Abazov *et al.* [D0 Collaboration], Phys. Rev. D **69**, 111101 (2004), [[arXiv:0308033](#)].
- [39] G. Aad *et al.* [ATLAS Collaboration], New J. Phys. **13**, 053044 (2011), [[arXiv:1103.3864](#)].
- [40] V. Khachatryan *et al.* [CMS Collaboration], Phys. Rev. Lett. **105**, 211801 (2010), [[arXiv:1010.0203](#)].
- [41] J. Zhu [ATLAS Collaboration], [SUSY '11 Plenary Talk].
- [42] B. A. Dobrescu, K. Kong, R. Mahbubani, JHEP **0707**, 006 (2007), [[arXiv:0703231](#)].
- [43] J. Alitti *et al.* [UA2 Collaboration], Z. Phys. **C49**, 17-28 (1991), [Journal Server].
- [44] T. Aaltonen *et al.* [CDF Collaboration], [[arXiv:1106.4782](#)].
- [45] V. M. Abazov *et al.* [D0 Collaboration], Phys. Rev. Lett. **101**, 221802 (2008), [[arXiv:0805.3556](#)].
- [46] M. A. Doncheski, R. W. Robinett, Phys. Rev. **D58**, 097702 (1998), [Journal Server].
- [47] CDF Collaboration, [W+ Higgs Limits].
- [48] D0 Collaboration, [W+ Higgs Limits].
- [49] ALEPH Collab., R. Barate *et al.*, Phys. Lett. **B495** (2000) 1, [[arXiv:0011045](#)].
- [50] L3 Collab., M. Acciarri *et al.*, Phys. Lett. **B495** (2000) 18, [[arXiv:0011043](#)].
- [51] OPAL Collab., G. Abbiendi *et al.*, Phys. Lett. **B499** (2001) 38, [[arXiv: 0101014](#)].
- [52] DELPHI Collab., P. Abreu *et al.*, Phys. Lett. **B499** (2001) 23, [[arXiv:0102036](#)].
- [53] J. Abdallah *et al.* [DELPHI Collaboration], Eur. Phys. J. C **51** (2007) 525, [[arXiv:0706.2741](#)].
- [54] G. Abbiendi *et al.* [OPAL Collaboration], Eur. Phys. J. **C33**, 463-476 (2004), [[arXiv:0308067](#)].
- [55] P. Achard *et al.* [L3 Collaboration], Phys. Lett. **B586**, 151-166 (2004), [[arXiv:0402036](#)].
- [56] T. Barklow *et al.* [ALEPH Collaboration], [Note 2001-060]
- [57] D. E. Kaplan, M. D. Schwartz, Phys. Rev. Lett. **101**, 022002 (2008), [[arXiv:0804.2477](#)].
- [58] B. Adeva *et al.* [L3 Collaboration], Phys. Lett. **B263**, 551-562 (1991), [Journal Server].
- [59] G. Abbiendi *et al.* [ OPAL Collaboration ], Eur. Phys. J. **C20**, 601-615 (2001), [[arXiv:0101044](#)].
- [60] P. Abreu *et al.* [ DELPHI Collaboration ], Phys. Lett. **B456**, 322-340 (1999), [Journal Server] .
- [61] A. Heister *et al.* [ALEPH Collaboration], Eur. Phys. J. **C27**, 1-17 (2003), [Journal Server].
- [62] S. Bethke, A. Ricker, P. M. Zerwas, Z. Phys. **C49**, 59-72 (1991), [Journal Server].
- [63] S. Bethke, Eur. Phys. J. **C64**, 689-703 (2009), [[arXiv:0908.1135](#)].
- [64] F. Cuyppers, A. F. Falk, P. H. Frampton, Phys. Lett. **B259**, 173-174 (1991), [Journal Server].
- [65] F. Cuyppers, P. H. Frampton, Phys. Rev. Lett. **63**, 125-127 (1989), [Journal Server].
- [66] K. G. Chetyrkin, Acta Phys. Polon. **B28**, 725-738 (1997), [[arXiv:9610531](#)].
- [67] K. Nakamura *et al.* [ Particle Data Group Collaboration], J. Phys. G **G37**, 075021 (2010), [PDG Online].